Effect of Buffer Anions on Pearl-Necklace Morphology of Tertiary Amine-Containing Binary Heterografted Linear Molecular Bottlebrushes in Acidic Aqueous Buffers

*Ethan W. Kent, Evan M. Lewoczko, and Bin Zhao**

Department of Chemistry, University of Tennessee, Knoxville, Tennessee 37996, United States

* Corresponding author (B.Z.). Email: bzhao@utk.edu

Abstract. Molecular bottlebrushes can exhibit a multitude of distinct conformations under different conditions, and precise control of their morphology can facilitate better use of such materials in potential applications. Herein we report a study on the effect of buffer anions on the pearl-necklace morphology of linear binary heterografted molecular brushes consisting of pH-responsive poly(2-*N,N*-diethylamino)ethyl methacrylate) (PDEAEMA) with a pK_a of 7.40 and thermoresponsive poly(ethoxydi(ethylene glycol) acrylate) (PDEGEA) with a lower critical solution temperature of 9 °C as side chains in various acidic aqueous buffers at 0 °C. The molecular brushes, denotated as BMB, were prepared by a grafting-to approach using copper(I)-catalyzed azide-alkyne cycloaddition reaction. Dynamic light scattering studies showed that the apparent hydrodynamic size of BMB in aqueous buffers with a pH of 6.50 at 1 °C decreased with increasing valency of buffer anions, from acetate anions with a charge of 1−, to phosphate anions carrying charges of 2− and 1−, and citrate anions bearing charges of 3− and 2− at pH = 6.50. Atomic force microscopy revealed that BMB exhibited a pearl-necklace morphology from all three aqueous buffers with a pH of 6.50 when spin cast at 0 °C. Analysis of AFM images showed that the average

length of BMB and the number of beads per brush molecule decreased with increasing valency of buffer anions while the size and height of the beads increased. The pearl-necklace morphology of BMB was believed to be the result of microphase separation of the neutral PDEGEA and the charged PDEAEMA side chains along the brush backbone. Multivalent buffer anions formed bridging linkages between protonated tertiary amine moieties and thus "crosslinked" the charged PDEAEMA side chains, resulting in shrinking of BMB and enhanced microphase separation of two side chain polymers.

Introduction

Molecular bottlebrushes (MBBs), also called molecular brushes or brush polymers, are a special class of graft copolymers in which relatively short polymeric side chains are densely end-tethered to a long backbone polymer via a covalent bond.[1-5] These complex polymers have garnered considerable attention in recent years due to their many unique features, including composition and topology versatility,[2] extremely high chain entanglement molecular weight,[6] large and tunable persistence length,[2] capability of shape changing in response to environmental variations,[2,3,7] and spontaneous symmetry breaking in crystallization at dilute conditions,[8] which originate from their distinctive molecular structures. In particular, MBBs can exhibit a multitude of distinct conformations according to environmental conditions,[2] and their large molecular sizes allow for facile visualization by atomic force microscopy (AFM) and transmission electron microscopy. In good solvents, molecular bottlebrushes with a high aspect ratio, determined by the chain lengths of backbone and side chain polymers, adopt stretched conformations and exhibit a cylindrical or wormlike shape due to the strong excluded volume interactions between adjacent side chains.[1-6] When the solvent quality changes, the brushes can assume different conformations, for example, globular.[2,3,7] MBBs have shown potential in many applications such as template synthesis of nanomaterials,[9] aqueous lubrication,[10] sensing,[11] drug delivery,[12] and fabrication of advanced polymeric materials (e.g., photonic crystals and supersoft elastomers).[6,13]

MBBs are generally synthesized using one, or a combination, of the following methods: grafting-from,[1-5,14-19] grafting-through,[12,20-22] and grafting-to.[23-27] Grafting-from is a process whereby side chains are grown from pendant initiating sites along the backbone polymer, typically via reversible deactivation radical polymerization such as atom transfer radical polymerization (ATRP). Grafting-through entails the polymerization of macromonomers to form MBBs directly,

typically via ring-opening metathesis polymerization using new generations of Grubb's catalyst.[20-22] Lastly, in the grafting-to process, pre-formed end-functionalized side chain polymers are covalently attached to a backbone polymer with complementary pendant functional groups.[23-27] The grafting-to method is versatile and allows for facile synthesis of heterografted molecular brushes containing two or more distinct side chain polymers. In addition, the backbone and side chain polymers are synthesized separately and can be thoroughly characterized prior to assembling them into brush polymers. With the use of click reactions, such as the copper(I)-catalyzed azide-alkyne cycloaddition (CuAAC) reaction, it has been shown that multicomponent MBBs with high and adjustable grafting densities can be readily synthesized by varying the ratio of backbone and end-functionalized side chain polymers.[23-27]

When a stimuli-responsive homopolymer is used as side chains and the aspect ratio of the backbone to the side chains is high, the formed MBBs can undergo drastic shape transitions in response to external stimuli.[2-4,27-41] For example, Li et al. observed that thermoresponsive poly(*N*-isopropylacrylamide) (PNIPAM) MBBs exhibited a worm-to-globule shape change upon heating from below to above the lower critical solution temperature (LCST) of PNIPAM.[28] However, the collapsed PNIPAM brushes were not stable and eventually precipitated from the solution. By introducing a second polymer into the side chains, either as a second type of side chains in binary heterografted brushes or as the outer block of diblock copolymer side chains in homografted MBBs,[27,38,39] we demonstrated the stabilization of collapsed stimuli-responsive MBBs against aggregation in solution. When a long stabilizing side chain polymer was employed, unimolecular worm-to-globule shape transitions were achieved in moderately concentrated aqueous solutions.[40] Moreover, when two different stimuli-responsive polymers were used as side chains for binary

heterografted three-arm star MBBs, two distinct collapsed globular states with different physicochemical properties were achieved from the same MBBs under different conditions.[41]

While studying the stimuli-induced star-globule shape transitions of dually responsive binary heterografted three-arm star MBBs (SBB) in aqueous solutions,[41] we observed a peculiar pearl-necklace structure of SBB by AFM. SBB was comprised of two side chain polymers with a 1-to-1 molar ratio: pH-responsive poly(2-(*N,N*-diethylamino)ethyl methacrylate) (PDEAEMA) with a pK_a of 7.4[41-43] and thermoresponsive poly(ethoxydi(ethylene glycol) acrylate) (PDEGEA) with an LCST of 9 °C.[44-47] The peculiar pearl-necklace morphology was observed when SBB was spin cast onto poly(methyl methacrylate) (PMMA)-coated mica from an aqueous phosphate buffer with a pH of 6.60 at 0 °C.[41] We hypothesized that the multivalent phosphate anions might form bridging linkages between protonated pendant tertiary amine groups in the PDEAEMA side chains, leading to and likely enhancing the microphase separation of PDEAEMA and PDEGEA side chains. To examine this hypothesis, we synthesized in the present work binary heterografted linear MBBs consisting of PDEAEMA and PDEGEA as side chain polymers (BMB) and studied the effect of buffer anions on their pearl-necklace morphology in acidic aqueous buffers. BMB was prepared by a grafting-to method in which alkyne end-functionalized PDEAEMA and PDEGEA homopolymers with a molar ratio of ~ 1 : 1 were grafted onto an azide-bearing backbone polymer via the CuAAC "click" reaction (Scheme 1). These side chain polymers and their molar ratio were chosen to closely mimic the composition of SBB for the previously observed pearl-necklace morphology. The behavior of BMB in aqueous acetate, phosphate, and citrate buffer solutions was investigated by dynamic light scattering (DLS) and AFM. While pearl-necklace nanostructures were observed for BMB in all three buffers, the number of beads per brush molecule decreased with increasing valency of buffer anions and the length, width, and height of beads increased. The

results from this study could offer a new perspective for pursuit of potential applications of MBBs such as template synthesis of nanoparticles.[1,4]

Scheme 1. Synthesis of Linear Heterografted Molecular Bottlebrushes Composed of PDEAEMA and PDEGEA Side Chains (BMB)

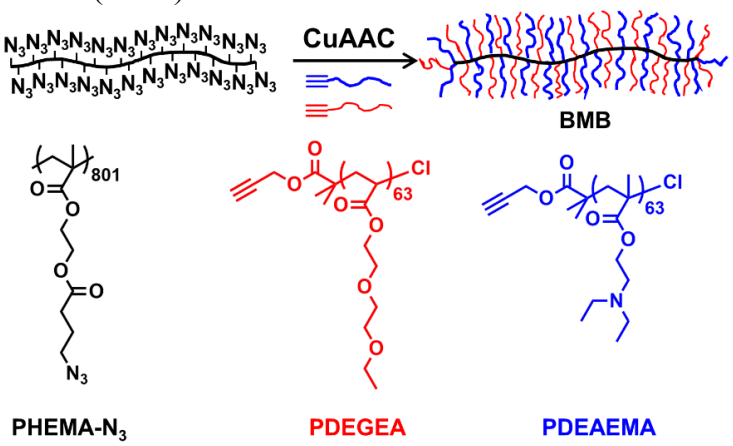

Experimental Section

Materials. 2-Bromoisobutyryl bromide (97%, Alfa Aesar), *N,N,N,N,N*-pentamethyldiethylenetriamine (PMDETA, 99%,Acros), 1,1,4,7,10,10-hexamethyltriethylenetetramine (HMTETA, 97%, Sigma-Aldrich), and 4-bromobutyryl chloride (95%, Acros) were purified by vacuum distillation. 2-(*N,N*-Diethylamino)ethyl methacrylate (DEAEMA, 98.5%, TCI) and ethoxydi(ethylene glycol) acrylate (DEGEA, 98%, TCI) were passed through a basic alumina (top)/silica gel (bottom) to remove the inhibitor prior to polymerization. Copper(I) chloride (CuCl, 99%, Sigma-Aldrich) was stirred in glacial acetic acid overnight, collected by vacuum filtration, washed thoroughly on the filter with absolute ethanol followed by diethyl ether, and then dried under high vacuum. 2-(Trimethylsilyloxy)ethyl methacrylate (HEMA-TMS) was synthesized by the reaction of 2-hydroxyethyl methacrylate with chlorotrimethylsilane and purified by vacuum distillation; the molecular structure of HEMA-TMS was confirmed by ^{1}H NMR spectroscopy. Propargyl 2-bromoisobutyrate (PBiB) were synthesized

according to a procedure described in the literature.[27] The detailed synthesis and characterization of PHEMA-N_3 with a degree of polymerization (DP) of 801, alkyne end-functionalized PDEGEA with a DP of 63, and alkyne end-functionalized PDEAEMA with a DP of 63 (Scheme 1) can be found in the Supporting Information. All other chemicals were purchased from either Sigma-Aldrich or Fisher and used as received.

General Characterization. ^{1}H NMR spectra were recorded on either a Varian VNMRS 500 or 600 spectrometer and the residual solvent peak was used as the reference. Size exclusion chromatography (SEC) of alkyne end-functionalized side chain polymers, PDEGEA and PDEAEMA, was conducted at ambient temperature using a PL-GPC 20 (an integrated GPC/SEC system from Polymer Laboratories, Inc.) with a differential refractive index (RI) detector, one PLgel 5 μm guard column (50 × 7.5 mm, Agilent Technologies), and two PLgel 5 μm mixed-C columns (each 300 × 7.5 mm, linear range of molecular weights from 200 to 2 000 000 Da, Agilent Technologies). The eluent was tetrahydrofuran (THF), with a flow rate of 1.0 mL/min, and the system was calibrated using a set of narrow disperse linear polystyrene standards (Scientific Polymer Products, Inc.). SEC analysis of the azide-bearing backbone polymer, PHEMA-N_3, and its precursors, PHEMA-TMS and PHEMA-Br, was carried out at 50 °C using a PL-GPC 50 Plus system (an integrated GPC/SEC system from Polymer Laboratories, Inc.) equipped with an RI detector, one PSS GRAL 10 μm guard column (50 × 8 mm, Polymer Standards Service-USA, Inc.) and two PSS GRAL 10 μm linear columns (each 300 × 8 mm, Polymer Standards Service-USA, Inc., linear range of molecular weight from 500 to 1 000 000 Da). The mobile phase was *N,N*-dimethylformamide (DMF) containing 50 mM LiBr at a flow rate of 1.0 mL/min, and the system was calibrated using a set of narrow disperse polystyrene standards (Scientific Polymer Products, Inc.). SEC analysis of the absolute molecular weight of BMB was performed using a GPC-MALS

system comprised of an Agilent model 1260 Infinity pump, a Rheodyne model 7725 manual injector with a 200 μL loop, and a Varian 390 LC detector system consisting of an RI detector and a dual angle light scattering detector (15° and 90°). The column set used consisted of one PSS GRAM 10 μm guard column (8 × 50 mm, PSS-USA, Inc.) and three PSS GRAM 10 μm linear columns (each 8 × 300 mm; 100, 1000, and 3000 Å, PSS-USA, Inc.). The analysis was conducted at 50 °C using DMF containing 0.1 M LiBr as eluent.

Dynamic Light Scattering (DLS) Study of BMB in Aqueous Solution. DLS experiments were carried out using a Malvern Zetasizer Nano ZS instrument equipped with a He-Ne 633 nm laser and a temperature controller at a scattering angle of 173°. Each DLS sample was prepared by transferring a known amount of BMB to a 20 mL scintillation vial from a stock solution in THF. The solvent was removed under high vacuum and the desired buffer solution was added immediately to dissolve the bottlebrushes. The pH of the solution was adjusted to 6.00 in an ice/water bath using 0.1 M HCl while stirring, and the brushes were allowed to equilibrate in a refrigerator at 4 °C overnight to ensure complete dissolution. To study the effect of various buffer anions on the solution state of BMB, aqueous solutions were prepared with a bottlebrush concentration of 0.1 mg/g in aqueous acetate, phosphate, and citrate buffers with salt concentrations of 5 mM and 50 mM. Note that the salts used for the preparation of buffers were sodium acetate, potassium dihydrogen phosphate, and sodium citrate, respectively. The pH of each solution was adjusted to 6.50 in an ice/water bath using 0.1 M NaOH and 0.1 M HCl, monitored by an Accumet AB-15 pH meter (calibrated at 0 °C using standard buffer solutions with pH values of 4.01, 7.00, and 10.01), and equilibrated for 15 min with stirring. A portion of the solution was transferred to a DLS cuvette and placed into the DLS instrument with a pre-set temperature of 1 °C. The sample was equilibrated for an additional 5 min before measurements were performed.

Each reported DLS value was an average of three measurements, with each measurement comprised of at least 10 runs. All reported hydrodynamic sizes (D_h) are the z-average values.

AFM Study of BMB. AFM was performed on a Digital Instruments Multimode IIIa Scanning Probe Microscope in tapping mode under ambient conditions. Reflective Al-coated Si probes (Budget Sensors) with a nominal resonant frequency of 300 kHz and a force constant of 40 N/m were employed. Scotch tape was used to cleave a clean layer of mica disk (Ted Pella, Inc.), which was either used directly or coated with poly(methyl methacrylate) (PMMA). The PMMA-coated mica disks were prepared by placing three drops of a 2.5 wt% solution of PMMA (M_n = 54.9 kDa) in $CHCl_3$ onto the freshly cleaved disk and spinning the solution off at 3000 rpm to create a thin film. The aqueous solutions from DLS measurements were used immediately to prepare the samples for AFM by spin casting onto the PMMA-coated mica at 3000 rpm; the substrates and spin coating stage were cooled in a refrigerator at 4 °C prior to spin casting of the BMB solutions. AFM samples for BMB on bare mica were prepared by spin casting a dilute solution of BMB in THF at 3000 rpm onto freshly cleaved mica at room temperature.

Synthesis of BMB. PHEMA-N_3 (5.24 mg, 2.17×10^{-5} mol -CH_2N_3 assuming quantitative functionalization, delivered via addition of 160.8 mg of a stock solution in THF with a concentration of 32.6 mg/g), PDEAEMA (159.6 mg, 1.35×10^{-5} mol, delivered via 1.719 g of a stock solution in THF with a concentration of 92.81 mg/g), PDEGEA (168.2 mg, 1.40×10^{-5} mol, delivered via 1.028 g of a stock solution in THF with a concentration of 163.6 mg/g), THF (5 mL), and CuCl (2.0 mg, 2.0×10^{-5} mol) were added to a 20 mL scintillation vial with a magnetic stir bar and sealed with a rubber septum. After purging the headspace of the vial with nitrogen gas through needles for 15 min, PMDETA (5.0 μL, 4.2 mg, 2.4×10^{-5} mol) was injected. The purging with nitrogen gas was continued for an additional 15 min; the needles were removed and the

reaction proceeded at room temperature. After 24 h, propargyl benzyl ether (50 μL) was injected in an attempt to cap unreacted azide moieties. After the reaction mixture was stirred for an additional 2 h, the vial was opened to air and an aliquot was taken for SEC analysis to determine the grafting density. The mixture was diluted with methylene chloride (50 mL) and passed through a column of basic alumina (top)/silica gel (bottom); the column was flushed with additional methylene chloride (100 mL). The crude mixture was concentrated by rotary evaporation to ~ 2 mL. Six fractionations were performed by cooling the crude solution in methylene chloride in a dry ice/acetone bath followed by the slow addition of hexanes (6 mL) to remove the unreacted side chain polymers, yielding 142.0 mg of molecular bottlebrushes (BMB). The complete removal of unreacted side chain polymers was confirmed by SEC analysis using PSS GRAM columns with DMF containing 100 mM LiBr as eluent at 50 °C. The absolute weight-average molecular weight (M_w) was determined by a GPC-MALS system: $M_W = 8.70 \times 10^6$ Da and $Đ$ of 1.07.

Results and Discussion

Synthesis of Azide-Bearing Backbone Polymer PHEMA-N_3 and Side Chain Polymers. PHEMA-N_3 (Scheme 1), with a degree of polymerization (DP) of 801, was prepared according to Scheme 2 by using a procedure similar to that for the azide-functionalized star backbone polymer that we reported previously.[41] Firstly, ATRP of 2-(trimethylsilyloxy)ethyl methacrylate (HEMA-TMS) was performed from initiator ethyl 2-bromoisobutyrate to form the silyl ether-protected linear backbone polymer precursor, PHEMA-TMS. The DP of 801 was calculated from the monomer conversion (39.2%), determined by ^{1}H NMR spectroscopy analysis, and the initial monomer-to-initiator molar ratio (2043 : 1). Secondly, a one-pot reaction was conducted to remove the silyl-ether protecting moiety in each repeat unit and subsequently install an alkyl bromide

group, producing precursor PHEMA-Br. Lastly, a substitution reaction of PHEMA-Br with sodium azide was carried out in DMF at ambient temperature to replace the bromide groups with azide. The degree of azide functionalization was 96.7%, calculated from the ^{1}H NMR spectrum of purified PHEMA-N_3 using the ^{1}H NMR spectra of PHEMA-TMS and PHEMA-Br as references. The detailed synthetic procedures and the characterization data for the backbone polymer and its precursors are presented in the Supporting Information (Figures S1 and S2).

Scheme 2. Synthesis of Azide-Bearing Backbone Polymer PHEMA-N_3

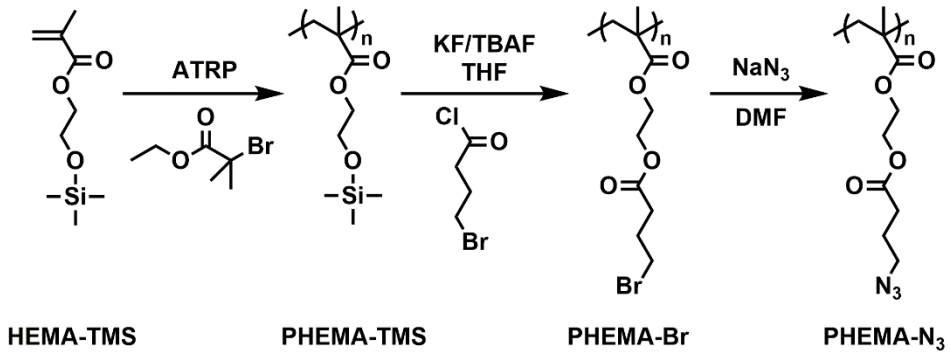

Alkyne end-functionalized thermoresponsive PDEGEA and pH-responsive PDEAEMA side chain polymers (Scheme 1) were made by ATRP. The polymerization of ethoxydi(ethylene glycol) acrylate (DEGEA) was carried out in anisole at 80 °C for 21 h using propargyl 2-bromoisobutyrate (PBiB) as initiator and CuCl/*N,N,N,N,N*-pentamethyldiethylenetriamine (PMDETA) as the catalyst/ligand. The molar ratios of $[DEGEA]_0$: $[PBiB]_0$: [CuCl] : [PMDETA] were 120 : 1 : 1 : 1.1. From SEC analysis, the polymerization of DEGEA was well controlled, resulting in a single, narrow molecular weight distribution with an $M_{n,SEC}$ of 12.1 kDa and a dispersity ($Đ$) of 1.17 (Figure S3A). The DP of the obtained PDEGEA was 63, calculated from the monomer conversion (52.5%), determined via ^{1}H NMR spectroscopy analysis by comparing the ester peaks of the

monomer (-COOCH_2-, 4.38-4.28 ppm) and the polymer (-COOCH_2-, 4.28-4.13 ppm), and the monomer-to-initiator ratio. The polymer was purified by passing through a basic alumina (top)/silica gel (bottom) column to remove the catalyst, followed by precipitation from THF into hexanes three times at room temperature. The ATRP of 2-(*N,N*-diethylamino)ethyl methacrylate (DEAEMA) was performed in anisole at 50 °C for 3.5 h using PBiB as initiator and CuCl/1,1,4,7,10,10-hexamethyltriethylenetetramine (HMTETA) as catalyst/ligand in the molar ratios of $[DEAEMA]_0 : [PBiB]_0 : [CuCl] : [HMTETA] = 120 : 1 : 1 : 1.2$. A lower temperature and a shorter polymerization time were used for ATRP of DEAEMA because the polymerization went much faster than that of DEGEA. SEC analysis of the obtained PDEAEMA revealed a single, narrow peak, with an $M_{n,SEC}$ of 13.6 kDa and $Đ$ of 1.13, indicating a well-controlled polymerization (Figure S3B). A DP of 63 was calculated using the monomer-to-initiator ratio and the monomer conversion (52.7%). The catalyst was removed using the same method as for PDEGEA, and the polymer was purified by repetitive precipitation from THF into hexanes at -78 °C in a dry ice/acetone bath.

Synthesis of Linear Binary Heterografted MBBs (BMB). BMB was synthesized by simultaneously attaching alkyne end-functionalized PDEGEA and PDEAEMA onto PHEMA-N_3 via CuAAC click reaction (Scheme 1). The reaction was carried out in THF at ambient temperature using CuCl/PMDETA as catalyst/ligand with a feed molar ratio of [PHEMA-N_3 repeat units] : [PDEGEA] : [PDEAEMA] = 1 : 0.65 : 0.62; an excess of side chains was used in order to achieve a high grafting density. After 24 h, propargyl benzyl ether was injected to attempt to cap unreacted azide groups. The copper catalyst was removed by passing the mixture through a column of basic alumina (top)/silica gel (bottom) and the bottlebrushes were purified by repeated fractionation in a mixture of methylene chloride and hexanes at -78 °C in a dry ice/acetone bath to remove

unreacted side chain polymers. The elimination of side chain polymers was confirmed by SEC analysis (Figure S4). ^{1}H NMR spectroscopy analysis of the purified bottlebrushes revealed that the composition of BMB was 51.6 mol % PDEGEA and 48.4 mol % PDEAEMA side chains, determined by comparing the integrals of the peaks at 4.33-4.11 ppm (-COOCH_2- of PDEGEA) and 4.11-3.91 ppm (-COOCH_2- of PDEAEMA) and using the DPs of the two polymers (Figure 1A). The overall grafting density of BMB was 72.5 %, calculated from the SEC peak areas of the brushes and the side chains, the feed ratios of backbone azide groups and two alkyne end-functionalized side chain polymers, and the molar ratio of PDEGEA and PDEAEMA side chains in the purified bottlebrushes. The details of calculation can be found in the Supporting Information. On average, there were 300 PDEGEA side chains and 281 PDEAEMA side chains (i.e., 1.77×10^4 tertiary amine groups) in each brush molecule.

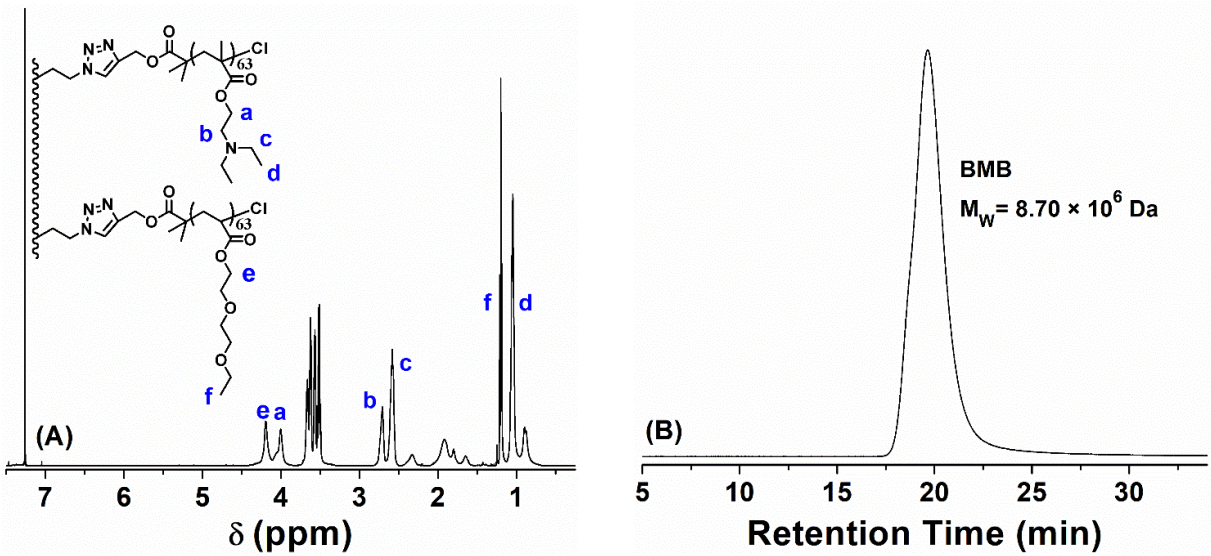

Figure 1. (A) ^{1}H NMR spectrum of the purified molecular bottlebrushes, BMB, in $CDCl_3$ and (B) size exclusion chromatography trace of BMB from a GPC-MALS system.

The absolute weight-average molecular weight (M_w) of BMB was found to be 8.70×10^6 Da using a GPC-MALS system equipped with an RI detector and a dual-angle light scattering detector

(Figure 1B). The calculated value of M_w for BMB was 8.19×10^6 Da, which was obtained by considering the weight-average molecular weight of PHEMA-N_3, the M_w of the side chain polymers ($M_n \times Đ$), and the grafting density from SEC peak areas. Thus, the calculated value of M_w was very close to the experimentally determined value by GPC-MALS, with a difference of 5.9% relative to the experimental M_w value. The formation of bottlebrushes was further confirmed by AFM imaging of the molecules spin cast onto freshly cleaved mica from a dilute solution in THF (Figures 2A and S5). The average length of the brush molecules, measured using the Image J software, was found to be 150 ± 47 nm and the typical height was ~ 1.5 nm (Figures S6 and 2B). Considering the contour length of the backbone (DP = 801) in an all-trans conformation, the average length measured from the AFM images corresponds to a degree of stretching of 74 %.

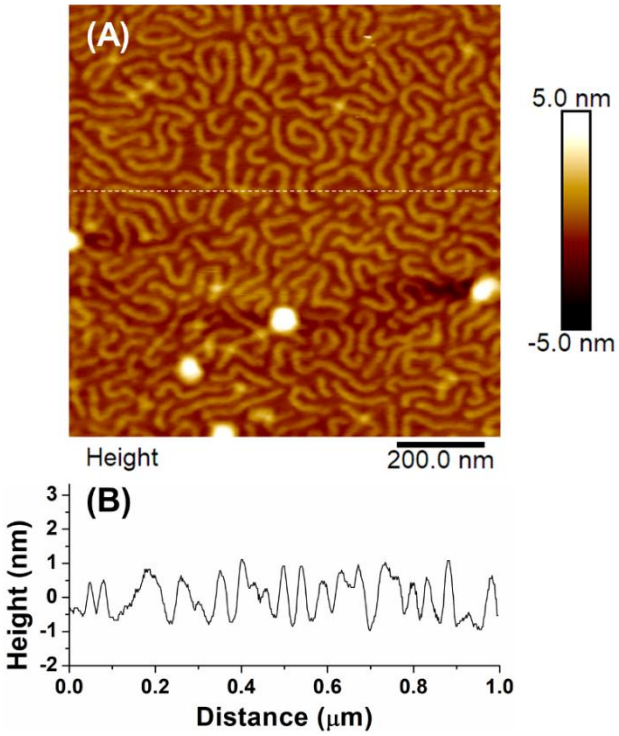

Figure 2. (A) AFM height image of BMB spin cast onto freshly cleaved bare mica from a 0.01 mg/g solution in THF. (B) Cross-sectional height profile along the dashed line in (A).

Dynamic Light Scattering (DLS) Study of BMB in Different Aqueous Buffer Solutions. DLS was used first to study the effect of buffer anions on the apparent hydrodynamic size or

diameter (D_h) of BMB in different aqueous buffer solutions. Note that the D_h value of a non-spherical nanoobject, such as a nanorod or wormlike MBBs, measured from DLS is the diameter of an equivalent sphere that has the same diffusion coefficient.[48,49] We hypothesized that higher valency buffer anions could form stronger bridging interactions between adjacent protonated PDEAEMA side chains, resulting in shrinking or partial collapse of the brush molecules. The aqueous solutions of BMB were prepared at a concentration of 0.1 mg/g in acetate, phosphate, and citrate buffers with salt concentrations of 5 and 50 mM, and the pH values for all the buffer solutions were adjusted to 6.50 at 0 °C in an ice/water bath. Calculations showed that the molar concentration of the tertiary amine groups of PDEAEMA in 0.1 mg/g aqueous solutions was 0.25 mM, significantly smaller than the buffer salt concentrations of 5 and 50 mM. While acetic acid exhibits one single pK_a at 4.74, phosphoric acid and citric acid each have three pK_a values (phosphoric acid: 2.14, 7.20, and 12.37; citric acid: 3.13, 4.76, and 6.40).[50] The LCST of PDEGEA is ~ 9 °C.[41,45] For comparison, the D_h of BMB in THF at a concentration of 0.1 mg/g at 25 °C was also measured and found to be 70.1 ± 0.1 nm with a polydispersity index (PDI) of 0.12 (Figure 3A). The small PDI suggested that the brush molecules were well dissolved in the solvent. For BMB in the 5 mM acetate buffer, the D_h was the largest observed, 78.0 ± 0.3 nm, with a single size distribution (PDI = 0.14) (Figure 3B), which indicated no intermolecular aggregation of brush molecules. This size was essentially the same as that observed for 0.2 mg/g BMB in water with a pH of 6.50 (D_h = 77.6 ± 0.6 nm and PDI = 0.20, see Figure S7; the small amount of large species observed in Figure S7 was likely the loosely associated brush molecules due to the absence of the buffer). At pH = 6.50, the acetate buffer exists in a nearly completely deprotonated state and the acetate anions bear a charge of 1−, while about 89% of tertiary amine pendant groups in PDEAEMA side chains are protonated with a charge of 1+, calculated based on the reported pK_a

value of 7.4 for PDEAEMA.[42] Therefore, the acetate ions could act as counter anions for the charged binary brushes, but could not form bridging interactions between adjacent protonated tertiary amine moieties. This led to high electrostatic repulsion between positively charged PDEAEMA side chains, causing the brushes to adopt an even more stretched conformation and thus exhibit a larger D_h than in THF. When the acetate buffer concentration was increased to 50 mM, the size decreased slightly to 74.9 ± 0.3 nm and the PDI was 0.14 (Figure S8A); this was due to the higher salt concentration that partially screened the electrostatic repulsive interactions between charged side chains, allowing the brushes to relax to a less stretched state.

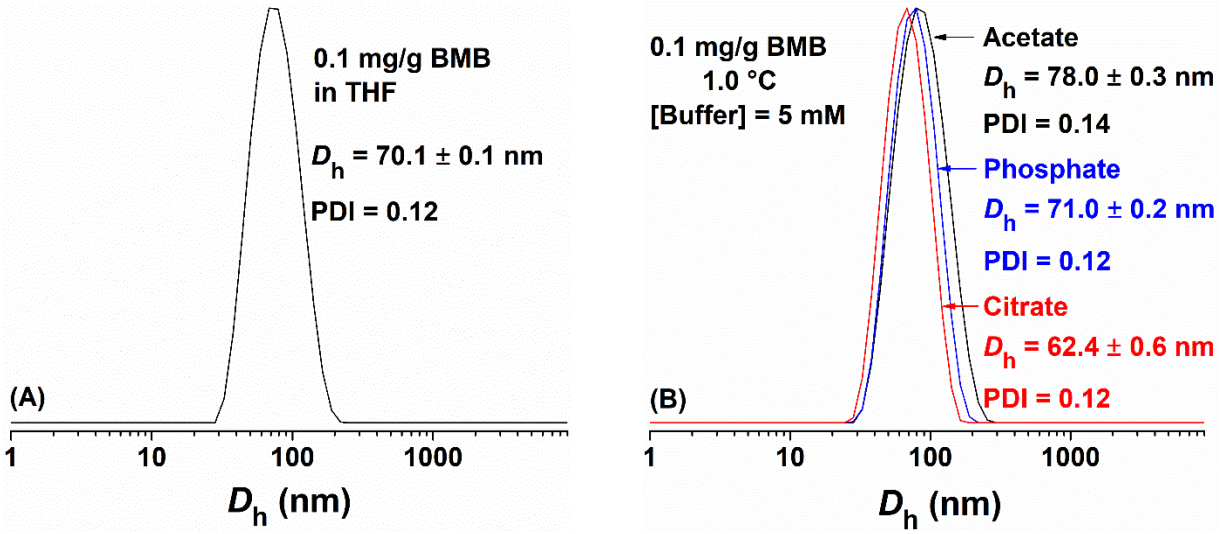

Figure 3. Hydrodynamic size distributions obtained from a DLS study of BMB at a concentration of 0.1 mg/g in (A) THF at 25 °C, and (B) 5 mM aqueous acetate, phosphate, and citrate buffer solutions with a pH of 6.50 at 1 °C.

For BMB in the 5 mM phosphate buffer solution, the D_h was found to be 71.0 ± 0.2 nm with a single size distribution (PDI = 0.12) (Figure 3B). This value is significantly lower than that of BMB in the 5 mM acetate buffer (78.0 nm) and is even appreciably smaller than in the 50 mM acetate buffer (74.9 nm, Figure S8A). According to the CurTiPot software,[51] about 30 % of phosphate anions at pH = 6.50 carried a charge of 2– and about 70 % carried a charge of 1–.

Calculations showed that the ionic strengths of the 5 mM acetate buffer, 50 mM acetate buffer, and 5 mM phosphate buffer solutions at pH = 6.50 are 5, 50, and 12.3 mM, respectively, and thus the ionic strength alone cannot explain the observations. This size decrease, compared to the acetate buffers, is likely due to the presence of divalent phosphate anions (HPO_4^{2-}) at pH = 6.50. The simultaneous interactions of one divalent phosphate anion with two protonated tertiary amine groups within one side chain or between adjacent side chains can be viewed as "crosslinking" of charged PDEAEMA side chains by divalent phosphate anions, which led to contraction of the bottlebrush molecules to a small hydrodynamic size. In the previous study of three-arm star MBBs with PDEGEA and PDEAEMA side chains (i.e., the SBB mentioned earlier), we observed that the D_h of SBB in a 10 mM phosphate buffer decreased slightly and gradually from 84.0 to 74.2 nm when the pH was increased from 5.00 to 7.96 before the drastic size reduction to 53.6 nm at pH 8.32.[41] The nearly 10 nm decrease in size was likely a combined result of decreased electrostatic repulsive interactions between protonated tertiary amine groups of PDEAEMA side chains and increased "crosslinking" by more multivalent phosphate anions with increasing pH. When the concentration of the phosphate buffer was increased to 50 mM, the D_h of BMB decreased slightly to 69.0 ± 0.4 nm with a PDI of 0.15 (Figure S8B). This decrease was likely caused by the increased salt concentration that screened electrostatic interactions between the protonated tertiary amine groups as in the case of the 50 mM acetate buffer and the increased bridging events due to more divalent HPO_4^{2-} counterions.

In the 5 mM citrate buffer at 1 °C, the hydrodynamic size of BMB decreased even further to 62.4 ± 0.5 nm, while a single size distribution was maintained (PDI = 0.12) (Figure 3B). At pH = 6.50, three distinct citrate anions exist in solution: about 55 % carrying a charge of 3–, 44 % bearing a charge of 2–, and 1 % carrying a charge of 1–.[51] The higher valencies and the larger

concentrations of tri- and divalent citrate anions, compared to phosphate anions at the same pH, led to more bridging events per citrate, resulting in further shrinking of the brush molecules. When the citrate concentration was increased to 50 mM, however, a small increase in D_h to 65.1 ± 0.6 nm (PDI = 0.13) was observed (Figure S8C, still < D_h = 69.0 nm in the 50 mM phosphate buffer. This observation is in line with the widely studied re-entrant behavior of polyelectrolyte chains with increasing the concentration of multivalent ions, that is, the charged polymer chains undergo conformational collapse or shrinking and then re-expansion with increasing the multivalent ion concentration.[52-54] This behavior is commonly attributed to the binding of multivalent ions to polymer chains and the overcompensation of the charges in the intermediate salt concentration region, resulting in charge inversion and consequently re-swelling.[52-55]

We note here that CH_3COO^-, HPO_4^{2-}, and citrate^{3-} are kosmotropic anions (water-structure makers),[55-61] which increase the order of water molecules surrounding them, while $H_2PO_4^-$ is borderline anion between water structure making and breaking according to Marcus.[56] We could not find from the literature whether citrate anion with a charge of 2- is kosmotropic or chaotropic, but mostly likely it is a kosmotrope, considering that citrate^{3-} is a stronger kosmotropic anion than HPO_4^{2-}.[57] On the other hand, K^+ is a weak structure-breaking cation, while Na^+ is a borderline ion; they are usually listed next to each other in the Hoffmeister series with somewhat similar properties in water.[56-60] Kosmotropic ions are known to exhibit "salting out" effects and decrease the cloud points of uncharged thermoresponsive polymers in water.[61-64] The buffer salt concentrations used here are rather low (5 and 50 mM), which we believe will not affect the cloud point of PDEGEA side chains much according to the literature reports. For example, Magnusson et al. reported that the cloud point of a thermoresponsive copolymer of two different oligo(ethylene glycol) methacrylates, a polymer similar to PDEGEA, in water decreased by < 1 °C when 50 mM sodium

acetate was added and by ~ 2 °C in the presence of 50 mM sodium sulfate.[63] Similar small decreases in the cloud point of poly(*N*-isopropylacrylamide) (< 2 °C) were reported by Zhang et al. in this low salt concentration region.[64] We previously observed by variable temperature ^{1}H NMR spectroscopy that the PDEGEA side chains of the aforementioned SBB in 10 mM phosphate buffers underwent LCST transitions in the temperature range of 10 – 13 °C at both pH 5.00 and 7.43.[41] Thus, we think that the PDEGEA side chains of BMB in 5 and 50 mM aqueous acetate, phosphate, and citrate buffers were in a soluble state at ~ 0 °C and our observations from DLS measurements were mainly due to the different valencies of buffer anions.

AFM Study of BMB from Aqueous Acetate, Phosphate, and Citrate Buffers. AFM was then employed to study the morphologies of BMB from the three aqueous buffer solutions. The 0.1 mg/g solutions of BMB in 5 mM buffers used in the DLS studies were directly spin cast onto poly(methyl methacrylate) (PMMA)-coated mica after DLS measurements. Figures 4A and B and S9 show the AFM height images of BMB on PMMA-coated mica spin cast from the 5 mM acetate buffer with a pH of 6.50 at ~ 0 °C (cooled in an ice/water bath). The brush molecules were in an extended worm-like state as expected because both side chain polymers were water-soluble at the aforementioned solution conditions. Image analysis showed an average contour length of 164 ± 44 nm (Figure S10), corresponding to a degree of stretching of 81% compared with the backbone in an all-trans zig-zag conformation. The average length was larger than that of the brushes from THF (150 nm ± 47 nm), consistent with the DLS measurement results (78.0 ± 0.3 nm in the 5 mM acetate buffer versus 70.1 ± 0.1 nm in THF). The molecular bottlebrushes here appeared to be more rigid than those cast from THF onto bare mica and displayed a rougher texture with small domains along the entire backbone length. As can be seen from Figure 4C, the height of the brushes undulated along the backbone direction, with height variations of ~ 1.5 nm. Thus, the overall

structure of BMB molecules was pearl-necklace-like, though the bead-like nanodomains were smaller and less pronounced than those we previously reported for SBB from a phosphate buffer.[41] The straighter pearl-necklace nanostructure of the brush molecules was most likely the result of microphase separation of the protonated PDEAEMA side chains and the neutral PDEGEA side chains with the incorporation of acetate anions in the positively charged PEAEMA nanodomains. Further image analysis showed that the average number of beads per brush molecule was 6.4 ± 2.0 (Figure S11), while the average longitudinal length of beads (along the brush backbone), the average lateral width (perpendicular to the backbone), and the height of the beads were 16.4 ± 5.0 nm (Figure S12), 14.7 ± 3.3 (Figure S13), and 2.4 ± 0.5 nm (Figure S14), respectively. The ratio of the average length to the average width of the beads was 1.1. These values are summarized in Table 1.

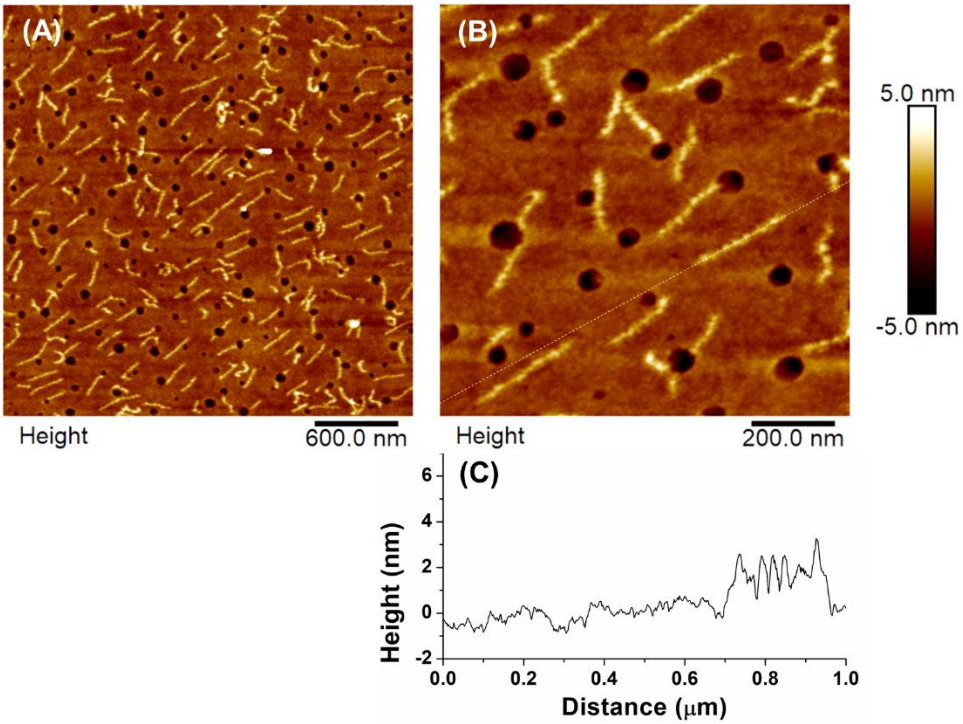

Figure 4. (A) and (B) AFM height images of brush molecules spin cast onto PMMA-coated mica from a 0.1 mg/g solution of BMB in a 5 mM acetate buffer with a pH of 6.50 at 0 °C. (C) Cross-sectional height profile along the dashed line in (B).

Table 1. Average length of BMB brush molecules, average number of beads per brush molecule, average longitudinal length of beads, average lateral width of beads, and average height of beads along with standard deviations from the analysis of AFM images of the brushes spin cast from 5 mM buffers using ImageJ and Nanoscope softwares.

Buffer	BMB Length (nm)	Number of Beads per Brush Molecule	Longitudinal Length of Beads (nm)	Lateral Width of Beads (nm)	Height of Beads (nm)
Acetate	164 ± 44	6.4 ± 2.0	16.4 ± 5.0	14.7 ± 3.3	2.4 ± 0.5
Phosphate	159 ± 45	4.5 ± 1.5	25.6 ± 6.8	15.4 ± 3.1	3.8 ± 0.6
Citrate	157 ± 42	3.8 ± 1.2	28.2 ± 7.1	20.7 ± 3.1	3.9 ± 0.7

Figures 5 and S15 show the AFM height images of BMB spin cast onto PMMA-coated mica from the 5 mM phosphate buffer with a pH of 6.50 at 0 °C. The brush molecules exhibited a pearl-necklace morphology composed of a number of bead-like nanodomains along the brush backbone, same as what we observed for SBB from a 5.0 mM phosphate buffer with pH = 6.60 at 0 °C.[41] Figure 5C shows the cross-sectional height profile along the brush backbone, where we can see that the height undulates along the contour of the brush molecule with approximately 2 – 3 nm variations. This is larger than the height variations of ~ 1.5 nm for the brush molecules from the acetate buffer (Figure 4C). Müller et al. previously reported by both AFM and TEM imaging similar pearl-necklace morphologies of linear core-shell homografted MBBs with diblock copolymer poly(acrylic acid)-*b*-poly(*n*-butyl acrylate) side chains,[65,66] where poly(acrylic acid) was the inner block, when multivalent metal cations (e.g., Fe^{3+} or Cd^{2+}) were incorporated into the core and complexed with the carboxylate anions or a bad solvent for the inner poly(acrylic acid) block was used. Using the two-gradient self-consistent field Scheutjens−Fleer (SCF-SF) approach and Monte Carlo (MC) simulations, Polotsky et. al. found that a decrease in the solvent quality from Θ to poor solvent conditions induced an instability in the cylindrically uniform nanostructure, resulting in the appearance of longitudinal undulations in the collapsed core of the molecular brushes.[67] Similar arguments can be applied to the complexation with multivalent metal cations.

Interestingly, our previous study showed that the linear brushes homografted with PDEAEMA-*b*-poly(methoxytri(ethylene glycol) acrylate) side chains, where PDEAEMA was the inner block, were rodlike with a uniform width and no height undulation along the backbone when the brush molecules were spin-cast from an aqueous phosphate buffer.[39] This suggests that other factors, such as grafting density, inner and outer block lengths, etc., may also play a role in the brush morphology.

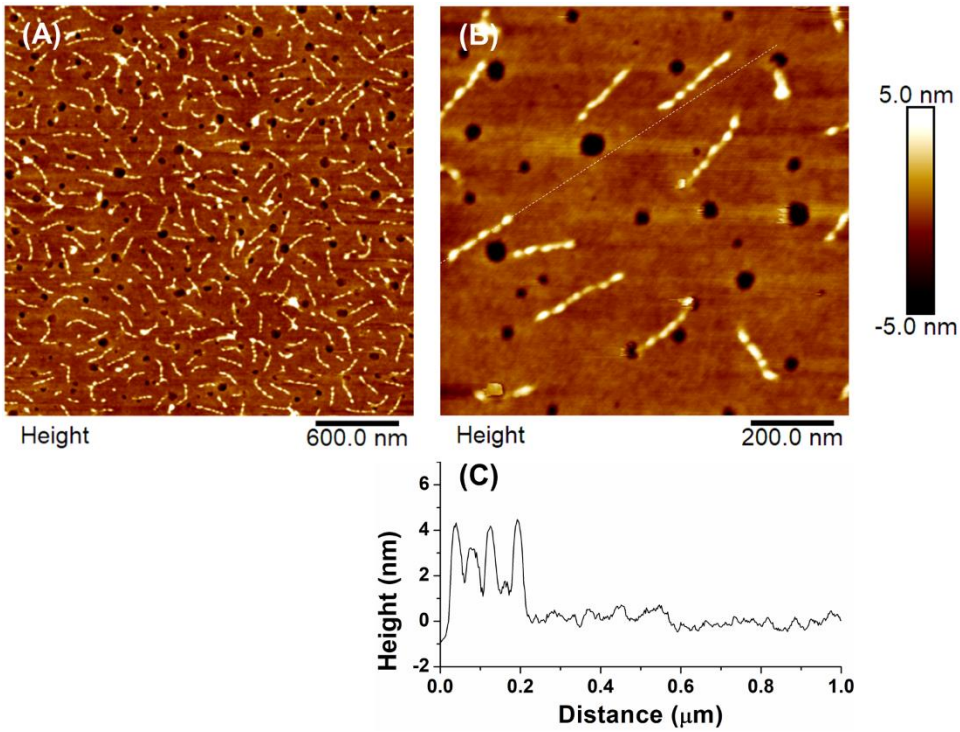

Figure 5. (A) and (B) AFM height images of BMB spin cast onto PMMA-coated mica from a 0.1 mg/g solution of BMB in a 5mM phosphate buffer with a pH of 6.50 at 0 °C. (C) Cross-sectional height profile along the dashed line in (B).

Analysis of the AFM images of BMB from the 5 mM phosphate buffer revealed that the average length was 159 ± 45 nm (Figure S16), which was slightly shorter than that from the acetate buffer (164 ± 44 nm) and represented a degree of stretching of 78 %. This is consistent with the observations from DLS measurements for the brushes in the two buffers (78.0 nm in the 5 mM acetate buffer vs 71.0 nm in the 5 mM phosphate buffer). The observation that the contour lengths

from AFM were closer to each other might be caused by the stretching effect when the brushes were spin cast onto the PMMA-coated mica. Despite this possible effect, we believe, based on other researchers' reports by both AFM and TEM[66] and our own experience, and that spin casting would not significantly alter the pearl-necklace morphology of the brushes or convert a uniform morphology to a pearl-necklace structure or vice versa. For example, we did not observe a pearl-necklace morphology for our previously reported homografted MBBs with PDEAEMA-containing diblock copolymer side chains spin cast onto PMMA-coated mica.[39] The average number of beads per brush molecule was 4.5 ± 1.5 (Figure S17), which decreased from 6.4 ± 2.0 for the acetate buffer. The average longitudinal length and lateral width were 25.6 ± 6.8 nm (Figure S18) and 15.4 ± 3.1 nm (Figure S19), respectively (Table 1). The aspect ratio of beads in the pearl-necklace structures, 1.7, was larger compared with the beads in the brushes from the acetate buffer, indicating a more elliptic shape for the beads. In addition, the bead height was greater, 3.8 ± 0.6 nm (Figure S20), compared with 2.4 ± 0.5 from the acetate buffer.

A similar but even more pronounced pearl-necklace morphology was observed for BMB spin cast from the 5 mM citrate buffer under the same conditions (Figures 6 and S21), with height undulations of 3-5 nm along the backbone. Analysis showed an average contour length of 157 ± 42 nm (Figure S22), which was slightly smaller than that from the 5.0 mM phosphate buffer (159 ± 45 nm). The number of beads per brush molecule decreased to 3.8 ± 1.2 (Figure S23), from 4.5 ± 1.5 for BMB from the 5.0 mM phosphate buffer solution, and the average longitudinal length, lateral width, and height of beads were 28.2 ± 7.1 nm (Figure S24), 20.7 ± 3.1 nm (Figure S25), and 3.9 ± 0.7 nm (Figure S26), respectively. The beads were slightly larger and taller than those observed from the phosphate buffer. These observations, along with a smaller hydrodynamic size from DLS measurements, suggest that the valency of the counterions plays an important role in

shaping the pearl-necklace morphology of binary heterografted MBBs.

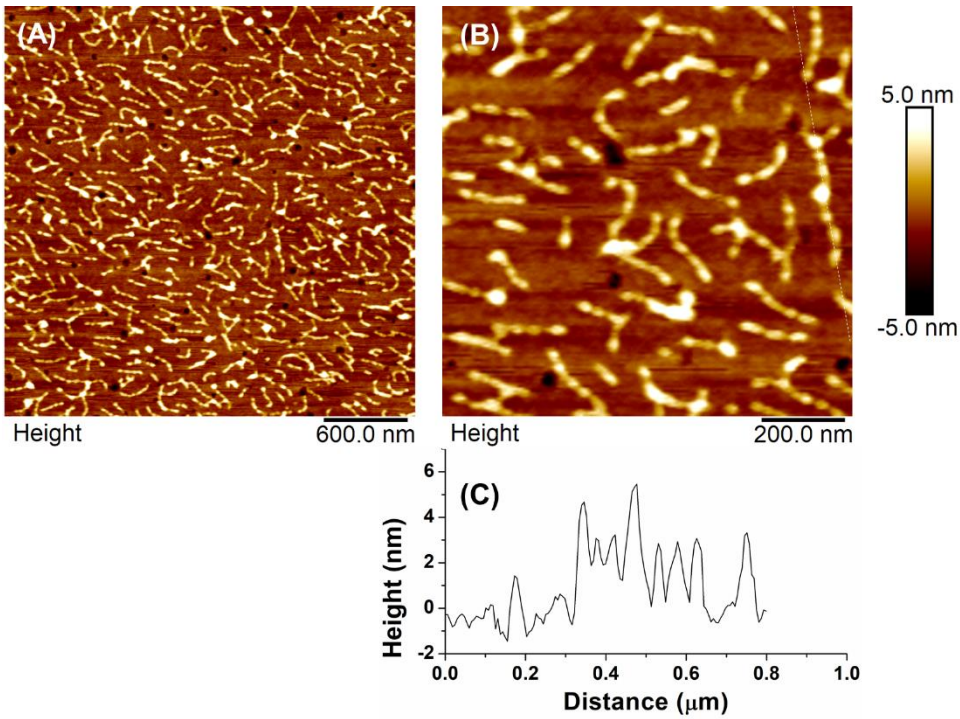

Figure 6. (A) and (B) AFM height images of BMB spin cast onto PMMA-coated mica from a 0.1 mg/g solution of BMB in a 5 mM citrate buffer with a pH of 6.50 at 0 °C. (C) Cross-sectional height profile along the dashed line in (B).

As can be seen from AFM images shown in Figures 4 – 6, binary heterografted BMB with PDEAEMA and PDEGEA side chains exhibited a pearl-necklace morphology from all three aqueous buffers with a pH of 6.50 at 0 °C. There was a clear trend that the DLS D_h, average contour length, and the number of beads per brush molecule decreased with increasing valency of buffer counteranions while the average length, width, and height of beads increased. The observed pearl-necklace morphology was most likely caused by the microphase separation of the neutral PDEGEA and the charged PDEAEMA side chains (Scheme 3). When the buffer contains divalent and/or trivalent anions, the local microphase separation of side chains along the brush backbone[68] is enhanced by the electrostatic bridging interactions (or "crosslinking") of the protonated tertiary amine groups within the same side chain and/or from adjacent PDEAEMA side chains by

multivalent buffer counter anions. This results in more pronounced pearl-necklace structures compared with monovalent buffer anions. Consequently, the number of beads per brush decreases, and the size and height of the beads increase. We previously observed that the homografted MBBs with PDEAEMA-containing diblock copolymer side chains spin cast from a pH 5.00 phosphate buffer were noticeably taller (~ 6 nm) than thermoresponsive MBBs (~ 1 nm) spin cast on the same type of substrate,[39] which was presumably caused by the incorporation of counteranions and possibly the additional salt. With this plus the current observation that the size and height of the beads increased from acetate to phosphate to citrate, it is reasonable to assign the beads as the PDEAEMA nanodomains in the microphase separated brush molecules (Scheme 3).

Scheme 3. Schematic Illustration of Microphase Separated Pearl-Necklace Structures of BMB with PDEGEA and Protonated PDEAEMA Side Chains at pH = 6.50 and T = 0 °C.

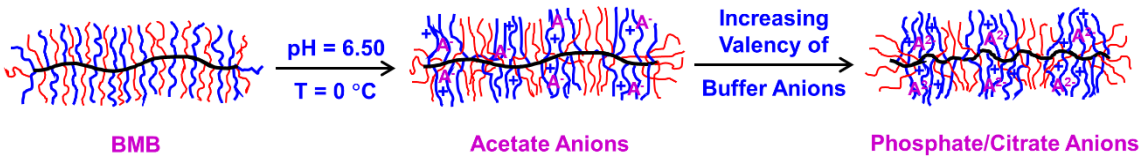

Conclusions

In summary, we synthesized linear binary heterografted molecular bottlebrushes consisting of PDEAEMA and PDEGEA side chains, BMB, by a click grafting-to method and investigated the effect of buffer anions on size and morphology of BMB in acidic aqueous buffer solutions at temperatures below the LCST of PDEGEA. DLS studies showed that under the same conditions the D_h of BMB in acidic buffer solutions decreased with increasing valency of the buffer anions, from acetate to phosphate and citrate. AFM revealed that BMB brush molecules spin cast onto PMMA-coated mica from all three buffers adopted a peculiar pearl-necklace morphology, with a

number of beads along the brush backbone for each buffer. Image analysis showed that the average contour length of the brushes and the number of beads per brush molecule decreased with increasing valency of buffer anions while the size and height of the beads increased. The smaller D_h values from DLS measurements and the larger sizes of bead-like domains of pearl-necklace nanostructures of BMB in the phosphate and citrate buffers are likely due to the di- and trivalent buffer anions forming bridging linkages between protonated tertiary amine moieties, resulting in shrinking of BMB and enhanced microphase separation of charged PDEAEMA and neutral PDEGEA side chains along the brush backbone. The effect observed in this work may facilitate the control in the template synthesis of nanomaterials by multicomponent bottlebrushes.

ORCID: Bin Zhao: 0000-0001-5505-9390

Supporting Information. Synthesis of PHEMA-N_3 and side chain polymers; characterization data for backbone polymer and its precursors and side chain polymers; SEC of BMB before and after the removal of side chains; DLS of BMB in 50 mM buffers; additional AFM images and image analysis; calculation of grafting density of BMB. The Supporting Information is available free of charge on the ACS Publications website at DOI: xxxxxxxxxxxxx.

Acknowledgements: This work was supported by NSF through DMR-1607076.

References:

1. Zhang, M.; Müller, A. H. E. Cylindrical polymer brushes. *J. Polym. Sci. Part A: Polym. Chem.* **2005,** *43*, 3461-3481.
2. Sheiko, S. S.; Sumerlin, B. S.; Matyjaszewski, K. Cylindrical molecular brushes: Synthesis, characterization, and properties. *Prog. Polym. Sci.* **2008,** *33*, 759-785.
3. Lee, H.-I.; Pietrasik, J.; Sheiko, S. S.; Matyjaszewski, K. Stimuli-responsive molecular brushes. *Prog. Polym. Sci.* **2010,** *35*, 24-44.
4. Yuan, J. Y.; Muller, A. H. E.; Matyjaszewski, K.; Sheiko, S. S. Molecular Brushes. In *Polymer Science: A Comprehensive Reference, 10 Volume Set*, Elsevier: 2012; Vol. 6, pp 199-264.

5. Xie, G.; Martinez, M. R.; Olszewski, M.; Sheiko, S. S.; Matyjaszewski, K. Molecular Bottlebrushes as Novel Materials. *Biomacromolecules* **2019,** *20*, 27-54.
6. Daniel, W. F.; Burdynska, J.; Vatankhah-Varnoosfaderani, M.; Matyjaszewski, K.; Paturej, J.; Rubinstein, M.; Dobrynin, A. V.; Sheiko, S. S. Solvent-Free, Supersoft and Superelastic Bottlebrush Melts and Networks. *Nat. Mater.* **2016**, *15*, 183−189.
7. Sheiko, S. S.; Prokhorova, S. A.; Beers, K. L.; Matyjaszewski, K.; Potemkin, I. I.; Khokhlov, A. R.; Möller, M. Single Molecule Rod−Globule Phase Transition for Brush Molecules at a Flat Interface. *Macromolecules* **2001**, *34*, 8354−8360.
8. Qi, H.; Liu, X. T.; Henn, D. M.; Mei, S.; Staub, M. C.; Zhao, B.; Li, C. Y. Breaking Translational Symmetry via Polymer Chain Overcrowding in Molecular Bottlebrush Crystallization. *Nature Communications* **2020**, *11*, 2152.
9. Zhang, M.; Drechsler, M.; Müller, A. H. E., Template-Controlled Synthesis of Wire-Like Cadmium Sulfide Nanoparticle Assemblies within Core−Shell Cylindrical Polymer Brushes. *Chem. Mater.* **2004,** *16*, 537-543.
10. Banquy, X.; Burdyńska, J.; Lee, D. W.; Matyjaszewski, K.; Israelachvili, J., Bioinspired Bottle-Brush Polymer Exhibits Low Friction and Amontons-like Behavior. *J. Am. Chem. Soc.* **2014,** *136*, 6199-6202.
11. Xu, H.; Sun, F. C.; Shirvanyants, D. G.; Rubinstein, M.; Shabratov, D.; Beers, K. L.; Matyjaszewski, K.; Sheiko, S. S., Molecular Pressure Sensors. *Adv. Mater.* **2007,** *19*, 2930-2934.
12. Johnson, J. A.; Lu, Y. Y.; Burts, A. O.; Xia, Y.; Durrell, A. C.; Tirrell, D. A.; Grubbs, R. H. Drug-Loaded, Bivalent-Bottle-Brush Polymers by Graft-through ROMP. *Macromolecules* **2010**, *43*, 10326−10335.
13 Liberman-Martin, A. L.; Chu, C. K.; Grubbs, R. H. Application of Bottlebrush Block Copolymers as Photonic Crystals. *Macromol. Rapid Commun.* **2017,** *38*, 1700058.
14. Matyjaszewski, K.; Qin, S.; Boyce, J. R.; Shirvanyants, D.; Sheiko, S. S., Effect of Initiation Conditions on the Uniformity of Three-Arm Star Molecular Brushes. *Macromolecules* **2003,** *36* (6), 1843-1849.
15. Runge, M. B.; Bowden, N. B., Synthesis of High Molecular Weight Comb Block Copolymers and Their Assembly into Ordered Morphologies in the Solid State. *J. Am. Chem. Soc.* **2007,** *129* (34), 10551-10560.
16. Xu, Y.; Bolisetty, S.; Drechsler, M.; Fang, B.; Yuan, J.; Ballauff, M.; Müller, A. X. E. pH and Salt Responsive Poly(*N,N*-dimethylaminoethyl methacrylate) Cylindrical Brushes and their Quaternized Derivatives. *Polymer* **2008**, *49*, 3957−3964.
17. Rzayev, J. Molecular Bottlebrushes: New Opportunities in Nanomaterials Fabrication. *ACS Macro Lett.* **2012**, *1*, 1146–1149.
18. Dai, W. X.; Zhu, X. M.; Zhang J.; Zhao, Y. L. Temperature and Solvent Isotope Dependent Hhierarchical Self-Assembly of a Heterografted Block Copolymer. *Chem. Commun.* **2019**, *55*, 5709–5712.
19. Zhu, X. M.; Zhang, J.; Miao, C.; Li, S. Y.; Zhao, Y. L. Synthesis, Thermoresponsivity and Multi-tunable Hierarchical Self-Assembly of Multi-Responsive $(AB)_mC$ Miktobrush-Coil Terpolymers. *Polym. Chem.* **2020**, *11*, 3003-3017.
20 Xia, Y.; Olsen, B. D.; Kornfield, J. A.; Grubbs, R. H. Efficient Synthesis of Narrowly Dispersed Brush Copolymers and Study of Their Assemblies: The Importance of Side Chain Arrangement. *J. Am. Chem. Soc.* **2009**, *131*, 18525−18532.

21. Li, Z.; Ma, J.; Cheng, C.; Zhang, K.; Wooley, K. L., Synthesis of Hetero-Grafted Amphiphilic Diblock Molecular Brushes and Their Self-Assembly in Aqueous Medium. *Macromolecules* **2010,** *43* (3), 1182-1184.
22. Levi, A. E.; Lequieu, J.; Horne, J. D.; Bates, M. W.; Ren, J. M.; Delaney, K. T.; Fredrickson, G. H.; Bates, C. M. Miktoarm Stars via Grafting-Through Copolymerization: Self-Assembly and the Star-to-Bottlebrush Transition. *Macromolecules* **2019**, *52*, 1794−1802.
23. Zhao, P.; Yan, Y.; Feng, X.; Liu, L.; Wang, C.; Chen, Y., Highly efficient synthesis of polymer brushes with PEO and PCL as side chains via click chemistry. *Polymer* **2012,** *53* (10), 1992-2000.
24. Tang, H.; Li, Y.; Lahasky, S. H.; Sheiko, S. S.; Zhang, D. Core−Shell Molecular Bottlebrushes with Helical Polypeptide Backbone: Synthesis, Characterization, and Solution Conformations. *Macromolecules* **2011**, *44*, 1491−1499.
25. Han, D.; Tong, X.; Zhao, Y. One-Pot Synthesis of Brush Diblock Copolymers through Simultaneous ATRP and Click Coupling. *Macromolecules* **2011**, *44*, 5531−5536.
26. Luo, H.; Szymusiak, M.; Garcia, E. A.; Lock, L. L.; Cui, H.; Liu, Y.; Herrera-Alonso, M. Solute-Triggered Morphological Transitions of an Amphiphilic Heterografted Brush Copolymer as a Single-Molecule Drug Carrier. *Macromolecules* **2017**, *50*, 2201−2206.
27. Henn, D. M.; Fu, W. X.; Mei, S.; Li, C. Y.; Zhao, B. Temperature-Induced Shape Changing of Thermosensitive Binary Heterografted Linear Molecular Brushes between Extended Worm-Like and Stable Globular Conformations. *Macromolecules* **2017**, *50*, 1645-1656.
28. Li, C.; Gunari, N.; Fischer, K.; Janshoff, A.; Schmidt, M. New Perspectives for the Design of Molecular Actuators: Thermally Induced Collapse of Single Macromolecules from Cylindrical Brushes to Spheres. *Angew. Chem., Int. Ed.* **2004**, *43*, 1101−1104.
29. Lee, H.-I.; Pietrasik, J.; Matyjaszewski, K. Phototunable Temperature-Responsive Molecular Brushes Prepared by ATRP. *Macromolecules* **2006**, *39*, 3914−3920.
30. Pietrasik, J.; Sumerlin, B. S.; Lee, R. Y.; Matyjaszewski, K. Solution Behavior of Temperature-Responsive Molecular Brushes Prepared by ATRP. *Macromol. Chem. Phys.* **2007**, *208*, 30−36.
31. Yamamoto, S.-i.; Pietrasik, J.; Matyjaszewski, K. ATRP Synthesis of Thermally Responsive Molecular Brushes from Oligo-(ethylene oxide) Methacrylates. *Macromolecules* **2007**, *40*, 9348−9353.
32. Lee, H.-I.; Boyce, J. R.; Nese, A.; Sheiko, S. S.; Matyjaszewski, K. pH-Induced Conformational Changes of Loosely Grafted Molecular Brushes Containing Poly(acrylic acid) Side Chains. *Polymer* **2008**, *49*, 5490−5496.
33. Xu, Y.; Bolisetty, S.; Ballauff, M.; Müller, A. H. E. Switching the Morphologies of Cylindrical Polycation Brushes by Ionic and Supramolecular Inclusion Complexes. *J. Am. Chem. Soc.* **2009**, *131*, 1640−1641.
34. Xu, Y.; Bolisetty, S.; Drechsler, M.; Fang, B.; Yuan, J.; Harnau, L.; Ballauff, M.; Müller, A. X. E. Manipulating Cylindrical Polyelectrolyte Brushes on the Nanoscale by Counterions: Collapse Transition to Helical Structures. *Soft Matter* **2009**, *5*, 379−384.
35. Gunari, N.; Cong, Y.; Zhang, B.; Fischer, K.; Janshoff, A.; Schmidt, M. Surfactant-Induced Helix Formation of Cylindrical Brush Polymers with Poly(L-lysine) Side Chains. *Macromol. Rapid Commun.* **2008**, *29*, 821−825.
36. Li, X.; ShamsiJazeyi, H.; Pesek, S. L.; Agrawal, A.; Hammouda, B.; Verduzco, R. Thermoresponsive PNIPAAM Bottlebrush Polymers with Tailored Side-Chain Length and End-Group Structure. *Soft Matter* **2014**, *10*, 2008−2015.

37. Kutnyanszky, E.; Hempenius, M. A.; Vancso, G. J. Polymer Bottlebrushes with a Redox Responsive Backbone Feel the Heat: Synthesis and Characterization of Dual Responsive Poly-(ferrocenylsilane)s with PNIPAM Side Chains. *Polym. Chem.* **2014**, *5*, 771−783.
38. Henn, D. M.; Lau, C. M.; Li, C. Y.; Zhao, B. Light-Triggered Unfolding of Single Linear Molecular Bottlebrushes from Compact Globular to Wormlike Nano-Objects in Water. *Polym. Chem.*, **2017**, *8*, 2702-2712.
39. Kent, E. W.; Henn, D. M.; Zhao, B. Shape-Changing Linear Molecular Bottlebrushes with Dually pH- and Thermo-Responsive Diblock Copolymer Side Chains. *Polym. Chem.* **2018**, *9*, 5133-5144.
40. Henn, D. M.; Holmes, J. A.; Kent, E. W.; Zhao, B. Worm-to-Sphere Shape Transition of Thermoresponsive Linear Molecular Bottlebrushes in Moderately Concentrated Aqueous Solution. *J. Phys. Chem. B* **2018**, *122*, 7015-7025.
41. Kent, E. W.; Zhao, B. Stimuli-Induced Star-Globule Shape Transitions of Dually Responsive Binary Heterografted Three-Arm Star Molecular Brushes in Aqueous Solution. *Macromolecules* **2019**, *52*, 6714-6724.
42. Zhou, K. J.; Wang, Y. G.; Huang, X. N.; Luby-Phelps, K.; Sumer, B. D.; Gao, J. M. Tunable, Ultrasensitive pH-Responsive Nanoparticles Targeting Specific Endocytic Organelles in Living Cells. *Angew. Chem. Int. Ed.* **2011**, *50*, 6109−6114.
43. Henn, D. M.; Wright, R. A. E.; Woodcock, J. W.; Hu, B.; Zhao, B. Tertiary Amine-Containing Thermo- and pH-Sensitive Hydrophilic ABA Triblock Copolymers: Effect of Different Tertiary Amines on Thermally Induced Sol-Gel Transitions. *Langmuir* **2014**, *30*, 2541–2550.
44. Hua, F. J.; Jiang, X. G.; Li, D. J.; Zhao, B. Well-Defined Thermosensitive, Water-Soluble Polyacrylates and Polystyrenics with Short Pendant Oligo(ethylene glycol) Groups Synthesized by Nitroxide-Mediated Radical Polymerization. *J. Polym. Sci. Part A: Polym. Chem.* **2006**, *44*, 2454-2467.
45. Jin, N. X.; Woodcock, J. W., Xue, C. M.; O'Lenick, T. G.; Jiang, X. G.; Jin, S.; Dadmun, M. D.; Zhao, B. Tuning of Thermo-Triggered Gel-to-Sol Transition of Aqueous Solution of Multi-Responsive Diblock Copolymer Poly(methoxytri(ethylene glycol) acrylate-*co*-acrylic acid)-*b*-poly(ethoxydi(ethylene glycol) acrylate). *Macromolecules* **2011**, *44*, 3556-3566.
46. Woodcock, J. W., Jiang, X. G.; Wright, R. A. E.; Zhao, B. Enzyme-Induced Formation of Thermoreversible Micellar Gels from Aqueous Solutions of Multiresponsive Hydrophilic ABA Triblock Copolymers. *Macromolecules* **2011**, *44*, 5764-5775.
47. Jin, N. X.; Zhang, H.; Jin, S.; Dadmun, M. D.; Zhao, B. Shifting Sol-Gel Phase Diagram of A Doubly Thermosensitive Hydrophilic Diblock Copolymer Poly(methoxytri(ethylene glycol) acrylate-*co*-acrylic acid)-*b*-poly(ethoxydi(ethylene glycol) acrylate-*co*-acrylic acid) in Aqueous Solution. *Macromolecules* **2012**, *45*, 4790-4800.
48. Hiemenz, P. C.; Lodge, T. P. *Polymer Chemistry*, 2nd ed.; CRC Press: Boca Raton, FL, 2007.
49. Chancellor, A. J.; Seymour, B. T.; Zhao, B. Characterizing Polymer-Grafted Nanoparticles: From Basic Defining Parameters to Behavior in Solvents and Self-Assembled Structures. *Anal. Chem.* **2019**, *91*, 6391-6402.
50. Brown, T. L.; LeMay, H. E.; Bursten, B. E.; Murphy, C. J.; Woodward, P. M. *Chemistry: the Central Science*, 12th ed.; Prentice Hall, 2011.
51. Gutz, I. G. R. CutTiPot - pH and Acid-Base Titration Curves: Analysis and Simulation freeware, version 4.2. http://www.iq.usp.br/gutz/Curtipot_.html.

52. Hsiao, P.-Y., Luijten, E. Salt-Induced Collapse and Reexpansion of Highly Charged Flexible Polyelectrolytes. *Phys. Rev. Lett.* **2006**, *97*, 148301.
53. Kundagrami, A.; Muthukumar, M. Theory of Competitive Counterion Adsorption on Flexible Polyelectrolytes: Divalent Salts. *J. Chem. Phys.* **2008**, *128*, 244901.
54. Jia, P. X.; Zhao, J. Single Chain Contraction and Re-expansion of Polystyrene Sulfonate: A Study on Its Reentrant Condensation at Single Molecular Level. *J. Chem. Phys.* **2009**, *131*, 231103.
55. Yuan, H. Y.; Liu, G. M. Ionic Effects on Synthetic Polymers: from Solutions to Brushes and Gels. *Soft Matter*, **2020**, *16*, 4087-4104.
56. Marcus, Y. Effect of Ions on the Structure of Water: Structure Making and Breaking. *Chem. Rev.* **2009**, *109*, 1346–1370.
57. Kunz, W.; Henle, J.; Ninham, B. W. 'Zur Lehre von der Wirkung der Salze' (About the Science of the Effect of Salts): Franz Hofmeister's Historical Papers. *Curr. Opin. Colloid Interface Sci.* **2004**, *9*, 19–37.
58. Mazzini, V.; Craig, V. S. J. What is the Fundamental Ion-Specific Series for Anions and Cations? Ion Specificity in Standard Partial Molar Volumes of Electrolytes and Electrostriction in Water and Non-aqueous Solvents. *Chem. Sci.* **2017**, *8*, 7052–7065.
59. Moghaddam, S. Z.; Thormann, E. The Hofmeister Series: Specific Ion Effects in Aqueous Polymer Solutions. *J. Colloid Interface Sci.* **2019**, *555*, 615–635.
60. Willott, J. D.; Murdoch, T. J.; Humphreys, B. A.; Edmondson, S.; Wanless, E. J.; Webber, G. B. Anion-Specific Effects on the Behavior of pH-Sensitive Polybasic Brushes. *Langmuir* **2015**, *31*, 3707−3717.
61. Murdoch, T. J.; Humphreys, B. A.; Johnson, E. C.; Webber, G. B.; Wanless, E. J. Specific Ion Effects on Thermoresponsive Polymer Brushes: Comparison to Other Architectures. *J. Colloid Interface Sci.* **2018**, *526*, 429–450.
62. Badi, N. Non-Linear PEG-Based Thermoresponsive Polymer Systems. *Prog. Polym. Sci.* **2017**, *66*, 54-79.
63. Magnusson, J. P.; Khan, A.; Pasparakis, G.; Saeed, A. O.; Wang, W.; Alexander, C. Ion-Sensitive "Isothermal" Responsive Polymers Prepared in Water. *J. Am. Chem. Soc.* **2008**, *130*, 10852-10853.
64. Zhang, Y. J.; Furyk, S.; Bergbreiter, D. E.; Cremer, P. S. Specific Ion Effects on the Water Solubility of Macromolecules: PNIPAM and the Hofmeister Series. *J. Am. Chem. Soc.* **2005**, *127*, 14505-14510.
65. Zhang, M.; Estournès, C.; Bietsch, W.; Müller, A. H. E. Superparamagnetic Hybrid Nanocylinders. *Adv. Funct. Mater.* **2004**, *14*, 871−882.
66. Zhang, M.; Drechsler, M.; Müller, A. H. E. Template-Controlled Synthesis of Wire-Like Cadmium Sulfide Nanoparticle Assemblies within Core−Shell Cylindrical Polymer Brushes. *Chem. Mater.* **2004**, *16*, 537−543.
67. Polotsky, A.; Charlaganov, M.; Xu, Y.; Leermakers, F. A. M.; Daoud, M.; Müller, A. H. E.; Dotera, T.; Borisov, O. Pearl-Necklace Structures in Core−Shell Molecular Brushes: Experiments, Monte Carlo Simulations, and Self-Consistent Field Modeling. *Macromolecules* **2008**, *41*, 4020–4028.
68. Theodorakis, P. E.; Paul, W.; Binder, K. Interplay between Chain Collapse and Microphase Separation in Bottle-Brush Polymers with Two Types of Side Chains. *Macromolecules* **2010**, *43*, 5137–5148

For TOC Graphic Only

Title: Effect of Buffer Anions on Pearl-Necklace Morphology of Tertiary Amine-Containing Binary Heterografted Linear Molecular Bottlebrushes in Acidic Aqueous Buffers

Authors: *Ethan W. Kent, Evan M. Lewoczko, and Bin Zhao*

TOC Graphic: